

# Assessment of Pseudorange Multipath at Continuous GPS Stations in Mexico

G. Esteban Vázquez<sup>1</sup>, Rick Bennett<sup>2</sup>, Joshua Spinler<sup>2</sup>

<sup>1</sup>Faculty of the Earth and Space Sciences, The Autonomous University of Sinaloa, Culiacan, Mexico; <sup>2</sup>Department of Geosciences, The University of Arizona, Tucson, USA.  
Email: [estebanv\\_99@yahoo.com](mailto:estebanv_99@yahoo.com)

Received April 26<sup>th</sup>, 2013; revised May 24<sup>th</sup>, 2013; accepted June 7<sup>th</sup>, 2013

Copyright © 2013 G. Esteban Vázquez *et al.* This is an open access article distributed under the Creative Commons Attribution License, which permits unrestricted use, distribution, and reproduction in any medium, provided the original work is properly cited.

## ABSTRACT

We conducted a study to quantify the amount of pseudorange multipath at continuous Global Positioning System (CGPS) stations in the Mexican territory. These CGPS stations serve as reference stations enabling rapid high-precision three-dimensional positioning capabilities, supporting a number of commercial and public safety applications. We studied CGPS data from a large number of publicly available networks spanning Mexico. These include the RGNA (National Active Geodetic Network) administered by INEGI (National Institute of Statistics and Geography), the PBO network (Plate Boundary Observatory) funded by the National Science Foundation (NSF) and operated by UNAVCO (University NAVstar Consortium), the Southern California Integrated GPS Network (SCIGN), which is a collaboration effort of the United States Geological Survey (USGS), Scripps Institution of Oceanography and the Jet Propulsion Laboratory (JPL), the UNAM network, operated by the National Seismological System (SSN) and the Institute of Geophysics of the National Autonomous University of Mexico (UNAM), the Suominet Geodetic Network (SNG) and the CORS (Continuously Operating Reference Station) network, operated by the Federal Aviation Administration (FAA). We evaluated a total of 53 CGPS stations, where dual-frequency geodetic-grade receivers collected GPS data continuously during the period from 1994 to 2012. Despite carefully selected locations, all GPS stations are, to some extent, affected by the presence of signal multipath. For GPS network users that rely on pseudorange observables, the existence of pseudorange multipath could be a critical source of error depending on the time scale of the application. Thus, to identify the most and the least affected GPS stations, we analyzed the averaged daily root mean square pseudorange multipath variations (MP1-RMS and MP2-RMS) for all feasible satellites tracked by the CGPS networks. We investigated the sources of multipath, including changes associated with hardware replacement (*i.e.*, receiver and antenna type) and receiver firmware upgrades.

**Keywords:** Pseudorange; Multipath; GPS; Network

## 1. Introduction

CGPS sites from the RGNA, PBO, SCIGN, UNAM, SNG and CORS networks considered in this study are located throughout the Mexican territory. All of these stations operate continuously, serving as reference stations for high-precision three-dimensional geodetic positioning applications based on GPS measurements. These reference stations are administered by a variety of organizations, including government agencies and public universities, and thus serve a wide range of positioning needs. Despite the diversity of the networks and their intended audiences, a core function of all of the networks is to provide a stable framework for high-precision positioning in support of diverse commercial and scientific

applications. In addition, the geographic distribution of stations provides a nation-wide access to the International Terrestrial Reference Frame (ITRF). For real-time kinematic (RTK) and rapid static applications that depend on the pseudo-range observable, the accuracy with which a roaming user may locate their assets with respect to the ITRF may be limited by site-specific multipath. The issue is particularly critical for users depending on pseudorange measurements for “real-time” (or “near-real-time”) kinematic GPS positioning, where ambiguity resolution is a critical step. The pseudorange multipath assessment considered in this research was performed for a total of 53 stations (see **Figure 1**) that collected continuous GPS data, 24 hours per day, and 365 days of the



Figure 1. CGPS sites in the Mexican territory (Map-Microsoft Streets & Trips).

year. We estimated the averaged daily root mean square pseudorange multipath variations (MP1-RMS and MP2-RMS) using the TEQC program, described in [3], in order to characterize the performance of each CGPS reference station based on of the level of multipath.

In some cases our analysis of the most severely affected sites was aided by photographs which provided clues regarding the possible sources of pseudorange multipath. We anticipate that our preliminary results will improve understanding of pseudorange multipath errors for reference networks in Mexico. All GPS sites are affected to some extent by multipath effects, which arise when reflected GPS satellite signals reach the receiving antenna, interfering with and obscuring the direct signal used for precise positioning. This effect may vary slowly on a seasonal basis, or abruptly due to natural events such as snowfall. Different research studies of multipath effects and suitable processing techniques can be referred for example by [1,2,4,5,7,10,12-14]. These papers show that multipath errors are larger for pseudorange (up to several meters) than for carrier phases (usually, millimeter to centimeter level). Since the multipath effects depend on the satellite geometry and the surrounding environment of the GPS antenna (as well as the antenna type), the effect is practically the same after one sidereal day under similar atmospheric conditions. With the current GPS constellation, the entire satellite configuration repeats each day, advancing only about 4 minutes between two consecutive days. Thus, the positioning solution of data derived from the repetition of the GPS satellite constellation between two sidereal days ought to be affected by “systematic” time-correlated multipath error. In gen-

eral, this effect can be used to mitigate the multipath effect from the positioning time-series results [4,7,13]. Reference [6] was the first to evaluate the pseudo-range multipath for a great number of CGPS stations from the CORS network, to closely identify problematic sites, and to compare various GPS hardware (*i.e.*, receiver and antenna type) combinations. In addition, multipath may contain valuable information about the local environment. For example, [8,15] had used uncalibrated pseudorange multipath variations (incoming signals are reflected by the ground before reception by the GPS receiver) at a single GPS site in order to investigate soil moisture, snow, and vegetation fluctuations. Therefore, pseudorange multipath estimates may also serve as a source of environmental sensor data.

## 2. GPS Instrumentation and Data Availability

In general, the GPS hardware for the different GPS arrays in Mexico consists of dual-frequency 12-20 channel, geodetic-grade GPS receivers and antennas. However, the brand of GPS receivers used at most of the networks is Trimble 5700, Trimble NETRS and Ashtech-Z12 receivers. The most common GPS antennas are Trimble Zephyr Geodetic (TRM41249.00), Ashtech Geodetic (ASH700228D), Trimble Dorne Margolin (TRM59800.00) and Ashtech Dorne Margolin (ASH701945B\_M) both with Choke-Ring; these last two types of antennas are usually designed to reduce L1 multipath. **Table 1** illustrates the GPS data availability indicated by the number of days available per year for all the sites considered in the experiment, including the site lo-

**Table 1. GPS data availability for CGPS sites in Mexico (\* means these CGPS station have been replaced, \*\* means that IITJ is a cooperative station of the RGNA and x means no data available for that year).**

Four Cha. ID	Site Location	GPS Array	Days of GPS data available per year																			
			94	95	96	97	98	99	00	01	02	03	04	05	06	07	08	09	10	11	12	
CHET	Chetumal	RGNA	x	x	x	x	x	x	x	x	x	x	x	87	359	361	366	360	363	362	364	
CHI3	Chihuahua	RGNA	x	x	x	x	x	x	x	x	x	x	x	x	x	x	x	x	359	365	363	
COL2	Colima	RGNA	x	x	x	x	x	x	x	x	x	x	x	82	352	364	366	364	365	364	365	
CULI*	Culiacán	RGNA	x	269	242	286	131	x	85	261	216	347	x	364	353	193	x	x	x	x	x	
CULC	Culiacán	RGNA	x	x	x	x	x	x	x	x	x	x	x	x	x	x	x	x	358	353	363	
HER2	Hermosillo	RGNA	x	x	x	x	x	x	x	x	x	349	321	362	362	364	366	362	365	365	365	
CAM2*	Campeche	RGNA	x	x	x	x	x	x	x	x	x	x	x	86	361	359	346	x	x	x	x	
ICAM	Campeche	RGNA	x	x	x	x	x	x	x	x	x	x	x	x	x	x	x	x	359	362	365	
ICEP	Puebla	RGNA	x	x	x	x	x	x	x	x	x	x	x	x	x	x	x	x	343	346	315	
IDGO	Durango	RGNA	x	x	x	x	x	x	x	x	x	x	x	x	x	x	x	x	355	349	361	
IITJ**	Jalisco	RGNA	x	x	x	x	x	x	x	x	x	x	139	330	361	328	291	356	363	365	365	
IMIE	Ensenada	RGNA	x	x	x	x	x	x	x	x	x	x	x	x	x	x	x	x	x	x	342	
IMIP	Cd. Juárez	RGNA	x	x	x	x	x	x	x	x	x	x	x	x	x	x	x	x	313	361	360	
INEG	Aguascalientes	RGNA	x	x	x	x	282	245	166	305	81	x	x	91	353	363	366	361	365	363	363	
LPAZ*	La Paz	RGNA	340	336	295	321	344	299	149	x	254	360	352	364	358	362	364	359	365	365	x	
IPAZ	La Paz	RGNA	x	x	x	x	x	x	x	x	x	x	x	x	90	362	364	365	362	364	365	365
MERI	Mérida	RGNA	x	x	x	x	x	x	x	x	x	x	x	90	362	364	365	362	364	365	365	
MEXI	Mexicali	RGNA	198	274	264	x	321	235	277	338	200	226	210	361	347	363	366	364	358	365	365	
MTY2	Monterrey	RGNA	x	x	x	x	x	x	x	x	x	x	x	91	355	364	365	357	365	365	365	
OAX2	Oaxaca	RGNA	x	x	x	x	x	x	x	x	x	x	x	99	361	365	364	348	365	362	365	
TAMP	Tampico	RGNA	x	x	x	x	x	x	x	x	x	x	x	x	x	x	x	x	339	350	360	
TOL2	Toluca	RGNA	x	x	x	x	x	x	x	x	x	x	x	89	345	361	364	363	363	365	362	
UGTO	Guanajuato	RGNA	x	x	x	x	x	x	x	x	x	x	x	x	x	x	x	x	340	360	363	
UQRO	Querétaro	RGNA	x	x	x	x	x	x	x	x	x	x	x	x	x	x	x	x	x	351	360	
USLP	S. Luis Potosí	RGNA	x	x	x	x	x	x	x	x	x	x	x	x	x	x	x	x	327	352	363	
UVER	Veracruz	RGNA	x	x	x	x	x	x	x	x	x	x	x	x	x	x	x	x	x	x	229	
VIL2	Villahermosa	RGNA	x	x	x	x	x	x	x	x	x	x	x	x	x	x	x	x	341	363	358	
PALX	El Álamo	PBO	x	x	x	x	x	x	x	x	x	x	x	x	x	x	x	x	x	364	364	
PHJX	Cucapah	PBO	x	x	x	x	x	x	x	x	x	x	x	x	x	x	x	x	x	63	365	
PJZX	Sr. Juárez	PBO	x	x	x	x	x	x	x	x	x	x	x	x	x	x	x	x	x	323	363	
PLPX	Las Pintas	PBO	x	x	x	x	x	x	x	x	x	x	x	x	x	x	x	x	x	363	365	
PLTX	Las Tinajas	PBO	x	x	x	x	x	x	x	x	x	x	x	x	x	x	x	x	x	364	365	
PSTX	San Isidoro	PBO	x	x	x	x	x	x	x	x	x	x	x	x	x	x	x	x	x	364	364	
PTAX	Puerta Peak	PBO	x	x	x	x	x	x	x	x	x	x	x	x	x	x	x	x	x	244	365	
PTEX	Testerazo	PBO	x	x	x	x	x	x	x	x	x	x	x	x	x	x	x	x	x	248	364	
SG21	Teoloyucan	SNG	x	x	x	x	x	x	x	x	x	x	229	295	337	178	32	x	x	x	x	
OXEC	El Camarón	SNG	x	x	x	x	x	x	x	x	x	x	x	x	x	347	151	x	x	x	x	
UCOM	Manzanillo	SNG	x	x	x	x	x	x	x	x	x	x	x	x	x	326	134	x	x	x	x	
SA61	Navojoa	SNG	x	x	x	x	x	x	x	x	x	x	x	x	x	x	x	18	361	258	x	
CIC1	Cicese	SCIGN	x	x	x	x	x	x	x	x	x	x	x	x	25	353	359	346	x	x	x	
SPMX	S. P. Mártir	SCIGN	x	x	x	x	x	x	x	x	x	x	x	x	x	x	x	216	x	x	x	
USMX	U. de la Sierra	SCIGN	x	x	x	x	x	x	x	x	x	x	x	327	347	363	365	66	x	x	x	
YESX	Yecora	SCIGN	x	x	x	x	x	x	x	x	x	x	x	x	x	x	x	x	x	181	x	
GUAX	Isla Gpe.	SCIGN	x	x	x	x	x	x	x	x	344	179	360	90	x	x	x	x	x	x	x	
CORX	Cors. Island	SCIGN	x	x	x	x	x	x	38	310	356	159	363	161	x	x	x	x	x	x	x	
DOAR	Dos Arroyos	UNAM	x	x	x	x	x	x	x	x	x	284	365	291	280	65	91	59	x	x	x	
CAYA	Cayaco	UNAM	x	x	x	318	289	332	342	260	263	292	41	x	x	x	x	x	x	x	x	
YAIG	Yautepec	UNAM	x	x	x	x	x	182	245	216	151	243	144	x	x	x	x	x	x	x	x	
MMD1	Mérida	CORS	x	x	x	x	x	x	x	x	x	x	x	x	x	x	213	357	363	362	360	
MMX1	México D.F.	CORS	x	x	x	x	x	x	x	x	x	x	x	x	x	x	207	354	363	364	351	
MPR1	P. Vallarta	CORS	x	x	x	x	x	x	x	x	x	x	x	x	x	x	212	356	363	364	357	
MSD1	S. J. del Cabo	CORS	x	x	x	x	x	x	x	x	x	x	x	x	x	x	211	323	365	364	360	
MTP1	Tapachula	CORS	x	x	x	x	x	x	x	x	x	x	x	x	x	x	213	356	198	220	361	

cation and the GPS array they belong. Two sites of the RGNA network (LPAZ and MEXI) recorded data continuously since 1994. Of these two stations, only MEXI continues recording data up to date. LPAZ was replaced by the station IPAZ in 2012. Nine additional sites from the RGNA network (CHET, COL2, HER2, IITJ, INEG, MERI, MTY2, OAX2 and TOL2) recorded data continuously for eight to thirteen years and the remaining RGNA sites have recorded data for only one to four years. Sites that belong to PBO network (PALX, PHJX, PJZX, PLPX, PLTX, PSTX, PTAX and PTEX) recorded data for two to three years. There exist six sites (CIC1, CORX, GUAX, SPMX, USMX and YESX) that belong to the SCIGN network and three sites from the SNG array (OXEC, SA61 and UCOM) that recorded between one and six years of continuous data, but these sites are no longer operational. There are three sites (DOAR, CAYA and YAIG) from UNAM and another site (SG21) from SNG that recorded data for some periods between 1997 and 2009, but there are no data after 2009. Finally, there are five sites (MMD1, MMX1, MPR1, MSD1 and MTP1) from the FAA CORS in Mexico, which recorded continuous data from 2008.

### 3. Pseudorange Multipath Assessment

We used the TEQC software (Test of Quality Check) provided by UNAVCO, which based on linear combinations of the pseudo-range and carrier phase observations seems to be the best option for estimating the pseudorange multipath effect [3] and [6]. TEQC software is available for public use at [18] to estimate the daily root mean squared multipath variations for each of the 53 analyzed sites. The main specifications for the GPS data processing included the use of a 30-sec sampling rate and 10° elevation cut-off angle. In addition, we followed the pseudorange multipath approach described in [3,6,1619]. According to this approach, the inter-channel bias and the non-integer initial phase terms for the GPS satellite and the receiver were not accounted for in the one-way observation equations used for the multipath estimation. It is well known that the pseudorange and carrier phase measurements on  $L1$  and  $L2$  for a satellite  $k$  and a receiver  $i$  are given by:

$$P_{L1} = R + c[\Delta t^k - \Delta t_i] + I_{L1} + T + MP_{P1} \quad (1)$$

$$P_{L2} = R + c[\Delta t^k - \Delta t_i] + I_{L2} + T + MP_{P2} \quad (2)$$

$$\Phi_{L1} = R + c[\Delta t^k - \Delta t_i] + \lambda_{L1}N_{L1} - I_{L1} + T + MP_{\Phi_{L1}} \quad (3)$$

$$\Phi_{L2} = R + c[\Delta t^k - \Delta t_i] + \lambda_{L2}N_{L2} - I_{L2} + T + MP_{\Phi_{L2}} \quad (4)$$

where:  $P_{L1}$  and  $P_{L2}$ : pseudorange observations (in units of m),  $R$ : geometric distance between the satel-

lite and the receiver (m),  $c = 300,000$ : constant speed of light ( $\text{km} \cdot \text{s}^{-1}$ ),  $\Delta t^k$ : satellite clock correction (s),  $\Delta t_i$ : receiver clock correction (s),  $I_{L1}$  and  $I_{L2}$ : ionospheric range errors (m),  $T$ : tropospheric range error (m),  $N_{L1}$  and  $N_{L2}$ : integer ambiguities (cycles),  $MP_{P1}$ ,  $MP_{P2}$ ,  $MP_{\Phi_{L1}}$  and  $MP_{\Phi_{L2}}$ : pseudorange and carrier phase multipath, respectively (including the observational noise),  $\lambda_{L1} \approx 19$  and  $\lambda_{L2} \approx 24$ : wavelengths of the signals on  $L1$  and  $L2$  (cm),  $f_1 \approx 1.5754$  and  $f_2 \approx 1.2276$ : frequencies of signals  $L1$  and  $L2$  (GHz), respectively.

Taking advantage of the relationship between the ionospheric delay for  $L1$  and  $L2$  leads to:

$$I_{L2} = \alpha \cdot I_{L1} \quad (5)$$

With:  $\alpha = (f_1/f_2)^2$

Subtracting (4) from (3) gives:

$$\Phi_{L1} - \Phi_{L2} = \lambda_{L1}N_{L1} - I_{L1} + MP_{\Phi_{L1}} - \lambda_{L2}N_{L2} + I_{L2} - MP_{\Phi_{L2}} \quad (6)$$

Substituting (5) into (6), grouping and simplifying yields:

$$\frac{\Phi_{L1} - \Phi_{L2}}{[\alpha - 1]} = I_{L1} + \frac{\lambda_{L1}N_{L1} - \lambda_{L2}N_{L2}}{[\alpha - 1]} + \frac{MP_{\Phi_{L1}} - MP_{\Phi_{L2}}}{[\alpha - 1]} \quad (7)$$

Combining (7) with (3) to eliminate  $I_{L1}$  term, results in:

$$\begin{aligned} & \Phi_{L1} + \frac{\Phi_{L1} - \Phi_{L2}}{[\alpha - 1]} \\ &= R + c[\Delta t^S - \Delta t_R] + T + \lambda_{L1}N_{L1} \\ & \quad + \frac{\lambda_{L1}N_{L1} - \lambda_{L2}N_{L2}}{[\alpha - 1]} + MP_{\Phi_{L1}} + \frac{MP_{\Phi_{L1}} - MP_{\Phi_{L2}}}{[\alpha - 1]} \\ &= R + c[\Delta t^S - \Delta t_R] + T + b_1 + m_{\Phi_1} \end{aligned} \quad (8)$$

Equation (8) is a linear combination of observed  $L1$  and  $L2$  carrier phases, where the ambiguity bias term  $b_1$  is introduced as:

$$b_1 = \lambda_{L1}N_{L1} + \frac{\lambda_{L1}N_{L1} - \lambda_{L2}N_{L2}}{[\alpha - 1]} \quad (9)$$

While the phase multipath effect is now defined by:

$$m_{\Phi_1} = MP_{\Phi_{L1}} + \frac{MP_{\Phi_{L1}} - MP_{\Phi_{L2}}}{[\alpha - 1]} \quad (10)$$

Combining (3), (7) and (8) gives:

$$\begin{aligned} & P_{L1} - \left(1 + \frac{2}{[\alpha - 1]}\right)\Phi_{L1} + \left(\frac{2}{[\alpha - 1]}\right)\Phi_{L2} \\ &= MP_{P1} - \frac{\lambda_{L1}N_{L1} - \lambda_{L2}N_{L2}}{[\alpha - 1]} - b_1 + MP_{\Phi_{L1}} - 2m_{\Phi_1} \end{aligned} \quad (11)$$

The new ambiguity bias term is now defined by:

$$\begin{aligned} B_1 &= -\frac{\lambda_{L1}N_{L1} - \lambda_{L2}N_{L2}}{[\alpha - 1]} - b_1 \\ &= -\left(1 + \frac{2}{[\alpha - 1]}\right)\lambda_{L1}N_{L1} + \left(\frac{2}{[\alpha - 1]}\right)\lambda_{L2}N_{L2} \end{aligned} \quad (12)$$

And the new phase multipath effect is introduced as:

$$\begin{aligned} M_{\Phi_1} &= -[MP_{\Phi_{L1}} - MP_{\Phi_{L2}}] - m_{\Phi_1} \\ &= -\left(1 + \frac{2}{[\alpha - 1]}\right)MP_{\Phi_{L1}} + \left(\frac{2}{[\alpha - 1]}\right)MP_{\Phi_{L2}} \quad (13) \\ &= MP_{\Phi_{L1}} - 2m_{\Phi_1} \end{aligned}$$

The pseudorange multipath  $MP_1$  is then expressed as the linear combination from (11), namely:

$$\begin{aligned} MP_1 &= P_{L1} - \left(1 + \frac{2}{[\alpha - 1]}\right)\Phi_{L1} + \left(\frac{2}{[\alpha - 1]}\right)\Phi_{L2} \quad (14) \\ &= MP_{P1} + B_1 + M_{\Phi_1} \end{aligned}$$

Similar derivations are performed to express  $MP_2$  as a linear combination:

$$\begin{aligned} MP_2 &= P_{L2} - \left(\frac{2 \cdot \alpha}{[\alpha - 1]}\right)\Phi_{L1} + \left(\frac{2 \cdot \alpha}{[\alpha - 1]} - 1\right)\Phi_{L2} \quad (15) \\ &= MP_{P2} + B_2 + M_{\Phi_2} \end{aligned}$$

with  $MP_{P2}$ ,  $B_2$ , and  $M_{\Phi_2}$  are defined similarly to  $MP_{P1}$ ,  $B_1$ , and  $M_{\Phi_1}$ .

As mentioned before, multipath error in the pseudoranges is significantly larger (up to several meters) but unbiased, compared to carrier phases (millimeter to centimeter level) which are biased. Also, both types of GPS measurements are sensitive to the effects of the troposphere, ionosphere, satellite orbits, receiver position, and clocks. Thus, (14) removes all of these effects except for the carrier phase bias ( $B_1$ ), which is a constant, leaving one systematic error term. Random variations in (14) can be reduced by averaging  $MP_{P1}$  values for many satellites. Based on the above derivations, the averaged daily root mean square (MP1-RMS and MP2-RMS) were computed by means of (14) and (15) for all possible tracked satellites during each day at each GPS site included in the experiment.

#### 4. Results and Analysis

At present the RGNA network consists of 23 continuous GPS stations administered by INEGI plus one cooperative station, which is controlled by the Institute of Land Information from Jalisco (IITJ). We analyzed the pseudorange multipath for only 27 of the RGNA stations: 24 existing plus three decommissioned sites (CULI, CAM2 and LPAZ). The first RGNA station that we investigated

is the INEG site since it had experienced important changes of receiver and antenna type as well as receiver firmware upgrades. Furthermore, INEG is the only site that currently uses a Trimble choke ring antenna (see **Figure 2**). The first upgrade for the Ashtech Z12 receiver at this site occurred on August 21, 1999 [21]. Then, a change of receiver and antenna happened in February 2000 when the Ashtech Z12 was replaced by a Trimble 4700 receiver and the ASH700228A antenna was replaced by a TRM29659.00 antenna. Another swap of receivers took place in the middle of March, 2008, when the Trimble 4700 was replaced by the Trimble 5700 receiver, which continues recording data up to present. The antenna is mounted on a concrete pillar monument (**Figure 2**), which is a known source of pseudorange multipath e.g., [2]. **Figure 3** shows the evolution of GPS pseudorange multipath at INEG station. GPS hardware replacements at INEG's site clearly impact the pseudorange multipath estimates. Here, two significant improvements can be observed in the multipath results, one at the beginning of 2000 (receiver and antenna replacement) and the other one after mid-march 2008 (receiver replacement). That is, an evident drop of the MP1-RMS decreasing their values abruptly from 80 to 20 cm and



**Figure 2. Aguascalientes (INEG) station with choke-ring antenna, RGNA network. Date of photo February, 2000.**

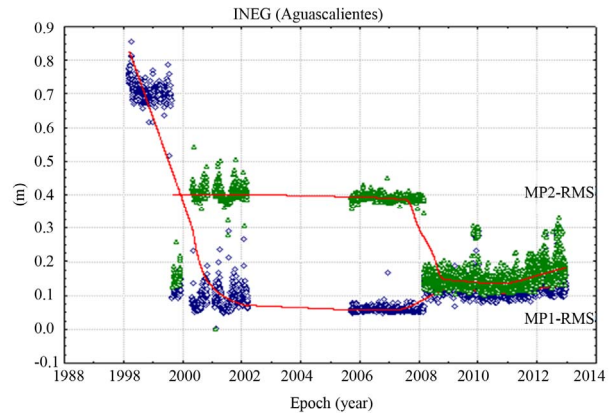


**Figure 3. Pseudorange multipath (MP1-RMS and MP2-RMS) variations at site INEG, RGNA network.**

also for the MP2-RMS from 50 to 20 cm, respectively. Additionally, there is no solution for the MP2-RMS before September 1999, since INEGI's receiver only recorded C/A code, which was used to generate the MP1-RMS.

**Figure 4** illustrates the pseudorange multipath (MP1-RMS and MP2-RMS) in terms of time-series for the three most contaminated (MEXI, CULI and LPAZ) and the three least affected (IPAZ, UVER and UGTO) RGNA sites. Large multipath RMS is evident in **Figures 4(a)-(c)**, where MP1-RMS values reach up to the meter level ( $\sim 3$  m), before 2000. Even though there were some upgrades to the receiver's firmware versions on August 1999 at MEXI and LPAZ and on September 2000 at CULI, only a solution for the MP1-RMS can be reported. Similarly to the data from site INEG, no P1 and P2 observables were available prior to 2000; however, the MP1-RMS results were generated based on the only available C/A code. These higher values of the MP1-RMS are likely attributable to the fact that the reported

C/A code is less accurate than the P1 code and possibly due to the receiver upgrades performed at that time. In addition, there was a change of receivers (Ashtech Z12 to a TRIMBLE 5700) and antennas (ASH700228A to a TRM41249.00) in January 2003 at MEXI, CULI and LPAZ stations, which might contribute to the observed drop in multipath RMS of about 50 cm. On the other hand, the less affected sites shown in **Figures 4(d)-(f)** ranged within 10 to 40 cm on both MP1-RMS and MP2-RMS variations. For the RGNA network, the most affected station on the MP1-RMS was MEXI, while the most affected on the MP2-RMS was site IITJ that uses an older TRIMBLE 4400 GPS receiver and a TRM23903.00 antenna, which never has been replaced since the installation of this site. It should be indicated that the three less affected sites from the RGNA use a modern Trimble Zephyr Geodetic rather than a Choke-Ring antenna (typically designed to mitigate L1 multipath). Panoramic photographs (taken in January 2003) of the three most affected RGNA sites are presented in **Figure 5** [21]; here

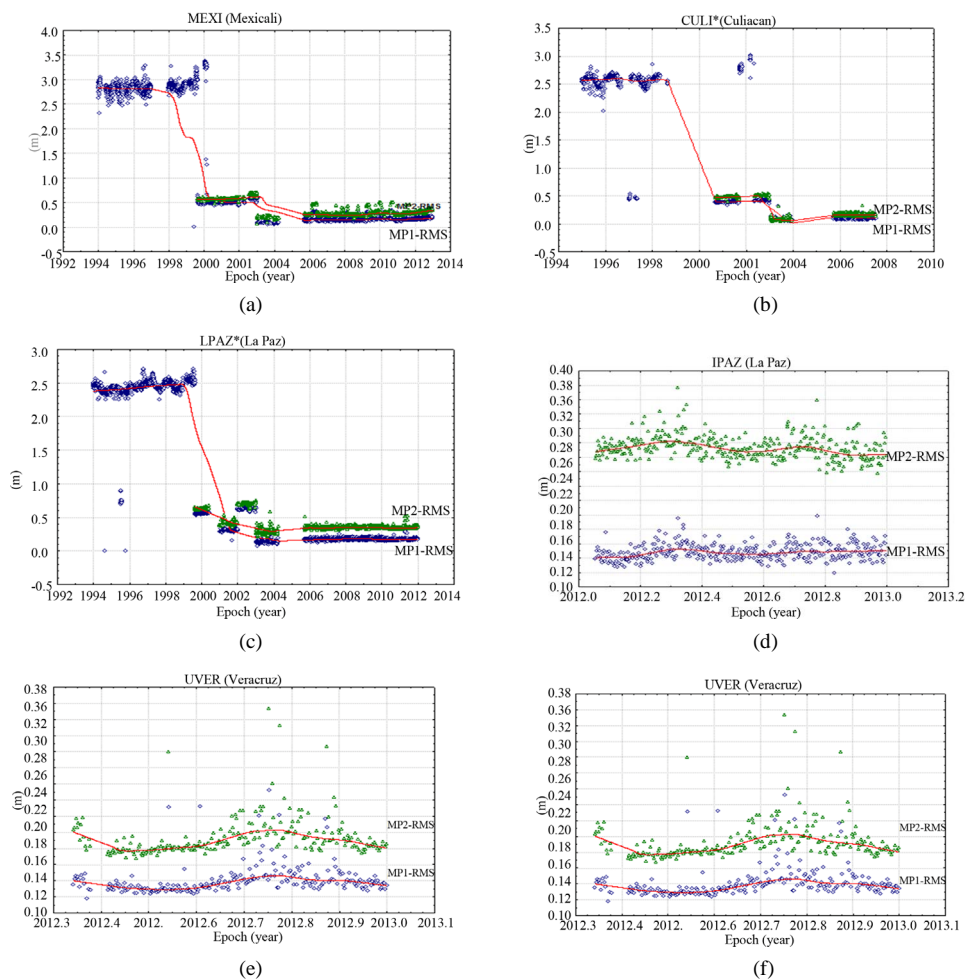


**Figure 4.** Pseudorange multipath MP1-RMS and MP2-RMS variations, most affected sites: (a) Mexicali (MEXI); (b) Culiacan (CULI); (c) La Paz (LPAZ) and least affected sites: (d) La Paz (IPAZ); (e) Veracruz (UVER); (f) Guanajuato (UGTO), RGNA network.



Figure 5. RGNA network sites: (a) Mexicali (MEXI), (b) Culiacán (CULI) and (c) La Paz (LPAZ).

it can be observed that the three antennas are placed on top of buildings and some local structures located in the surrounding antenna environment might be a potential source or contributor of the evident multipath existence. **Figure 6** presents the pseudorange multipath time-series for the most affected GPS sites (SA61, CIC1 and CORX), that are associated to SNG and SCIGN arrays. In **Figure 6(a)** variations for SA61 are within 40 to 50 cm, but with some disperse values (at the beginning of 2011) that can be attributed to some cause other than a change in hardware. There is not a convincing argument of what could cause these higher values around 2011. SA61 is found to be the most contaminated site of the SNG network as compared to SG21, OXEC and UCOM stations. An ascending trend on the pseudorange multipath variation results can be observed at the end of 2009 for CIC1 site as illustrated in **Figure 6(b)**. Unfortunately there is no more data after that year, with which to further investigate multipath at this station. Multipath at site CORX also exhibits unusual behavior; with the multipath RMS values dropping at the end of 2003, see **Figure 6(c)**. This drop may be attributed to a change in the antenna that occurred in mid November when the ASH701945B\_M was replaced by the ASH701945C\_M antenna; since no replacement on the GPS receiver is documented for this site.

**Figure 7** shows the three most (PHJX, PTEX and PLTX) and three least (PLPX, PTAX and PJZX) affected sites from the PBO network, respectively. The scatter for the most affected stations ranges from 25 to 50 cm, while less affected sites fluctuate between 20 and 30 cm. Even though, PLPX, PTAX and PJZX are the sites that experienced smallest amounts of pseudorange multipath effects (ranked over all PBO stations in Mexico) an evident annual behavior can be observed on the variation results at these sites. Panoramic pictures for the three most affected (PHJX, PTEX and PLTX) PBO sites are shown in **Figure 8**, courtesy of [20]. The antennas for the PBO stations are mounted on shallow-braced monuments in open fields, where the most likely source of multipath is the ground surface in the vicinity of the monuments. Reference [11] demonstrated that antenna height estimates and MP1-RMS or MP2-RMS variation time-series

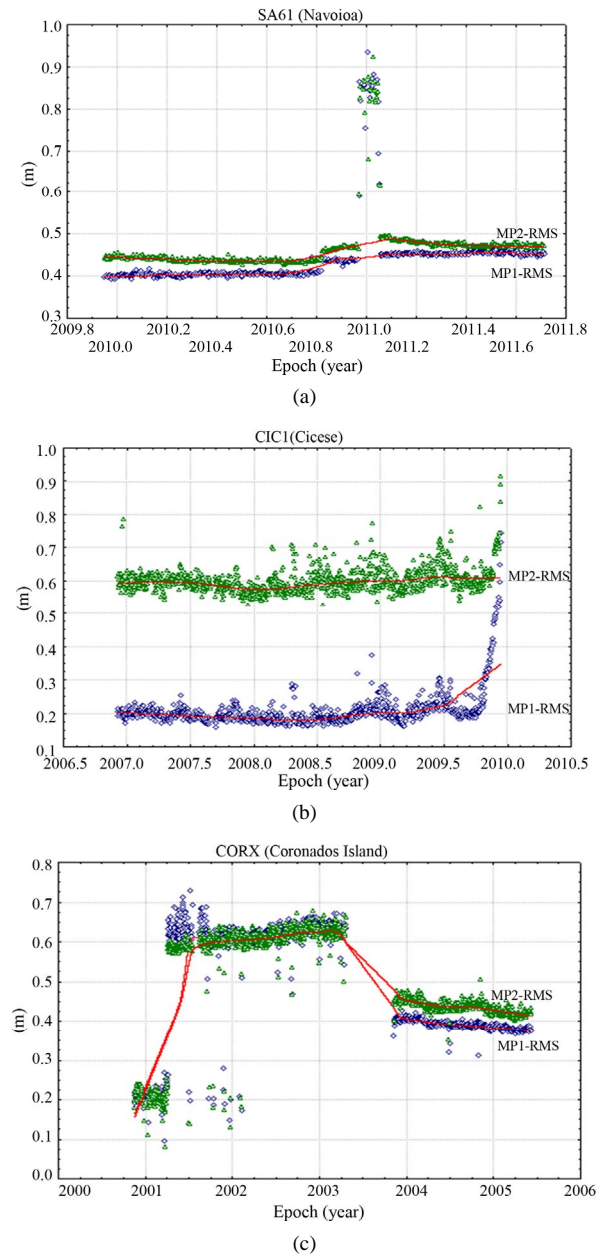
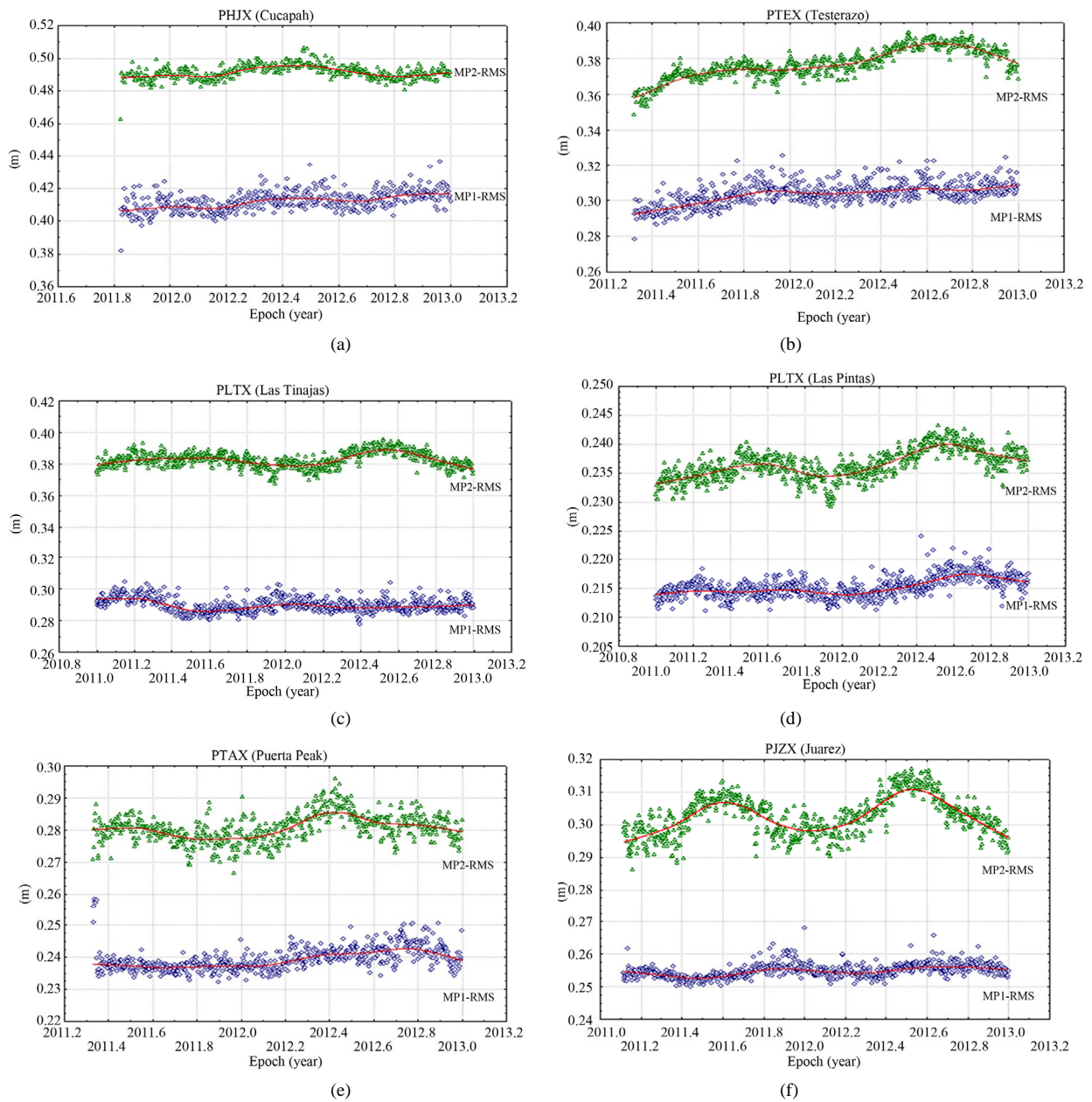
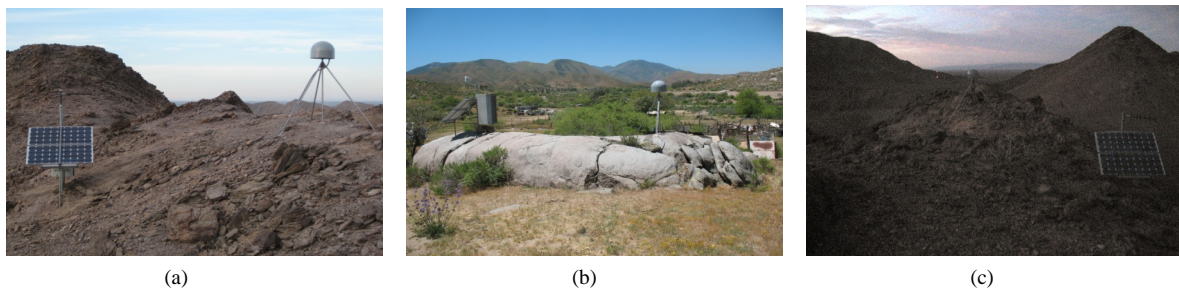


Figure 6. Pseudorange multipath MP1-RMS and MP2-RMS variations, most affected sites: (a) Navjoia (SA61), SNG network; (b) Cicese (CIC1), SCIGN network and Coronados Island (CORX), SCIGN network.



**Figure 7. Pseudorange multipath MP1-RMS and MP2-RMS variations, most affected sites: (a) Cucapah (PHJX); (b) Testerazo (PTEX); (c) Las Tinajas (PLTX) and least affected sites: (d) Las Pintas (PLPX); (e) Puerta Peak (PTAX); (f) Sr. Juárez (PJZX), PBO network.**



**Figure 8. PBO network: (a) HJ Cucapah (PHJX) site, date of photo October, 2011; (b) Testerazo (PTEX) site, date of photo April, 2011; Las Tinajas (PLTX) site, date of photo October, 2010.**

are highly correlated. This is illustrated for the Mexico PBO sites in **Figure 9**. Prominent annual variations are apparent in both the height and the MP2-RMS time series, coincident with one another. The peak values for height as well as for the MP2-RMS variations were encountered at the middle of 2011 and 2012, respectively. There are several possible explanations for this coincidence, including a potential instrumental response that may be attributed to some primary seasonal forcing, inappropriate modeling in the GPS data analysis, and the presence of the remaining multipath effects in the final positioning estimates. However, this fact needs further investigation

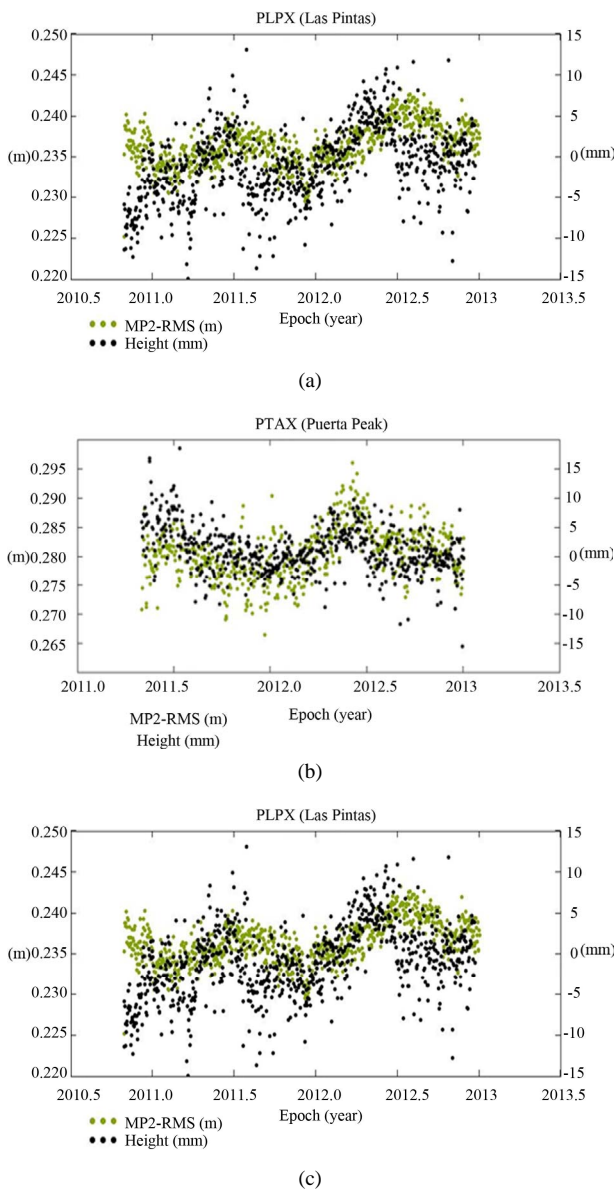


**Figure 9.** Time-series for height component (right scale in mm.) and MP2-RMS (left scale in m.), PBO network: (a) Las Pintas (PLPX) site; (b) Puerta Peak (PTAX) site; (c) Sr. Juarez (PJZX) site.

in order to demonstrate and understand more what is causing these coincidences.

Cayaco (CAYA) belongs to the GPS network from UNAM, and is located at the Pacific coast in the Guerrero region and it was the only continuous station in operation in 1998, allowing for the first detection of silent earthquake phenomena associated with the Middle America trench near Guerrero, Mexico [9]. CAYA is the only site considered in the experiment that uses a LEICA SR530 receiver and a TRIMBLE Geodetic L1/L2 (TRM22020.00) antenna. Comparing this site among to all the analyzed stations, CAYA was found to be one of the most affected sites. Even though, CAYA's results approximately range within 30 to 70 cm from 1997 to 2002. There is an evident jump immediately after that year reaching values up to 2.2 m, see **Figure 10(a)**. It is suspected that this fact might be attributed to a change in the hardware, since prior to 2002 CAYA used a TRIMBLE 4000SSE GPS receiver. However, a drop can be seen in the results at the end of 2003 and this issue may be attributed to an update in the firmware version of the LEICA SR530 GPS receiver from 4.01 to 4.22. Based on the GPS data availability, Yautepec (YAIG) is another station from the UNAM network considered in the experiment. It is located in the Morelos region and its main objective, since it was installed in 1999, is to investigate possible displacements associated with the slow slip event that first started sometime during mid-November to early December 2001 [17]. The MP1-RMS and MP2-RMS variations for this site are as high as 85 cm, see **Figure 10(b)**; ranked overall stations at sixth place. A gap in the data can be observed between 2001 and 2003 and part of 2004. There is no basis to argue that the drop of the results during these times can be attributed to any replacement in the hardware, since the same receiver (Ashtech Z-12) and antenna type (ASH700936E\_C) remained at this site from August 2002 up to the last date it recorded GPS data. Finally, results for the most affected site (MPR1) from the CORS network is illustrated in **Figure 10(c)**. Here, MPR1 site shows a scatter for both MP1-RMS and MP2-RMS that ranges roughly from 80 to 110 cm; that is why MPR1 site is ranked first among the other CORS sites and overall ranked fourth highest for MP1-RMS and third highest for MP2-RMS (see **Tables 2 and 3**) among all tested sites. **Tables 2 and 3** show the statistics (in units of centimeters) for the MP1-RMS and MP2-RMS variations at all tested GPS stations. The NGS designator for the type of GPS receiver and antenna used are included as well as the name of the station, the number of available days of data and the acronym of the array to which they belong. CGPS stations were ranked from the most to the least affected based on their max and min values. However, an important issue here is that all sites present a great variety of GPS data availability,

**Table 2. Statistics of the MP1-RMS variations for CGPS sites spanning Mexico.**

Rank (Order)	Site	No. of Days	Max (cm)	Min (cm)	Mean (cm)	St. Dev. $\pm$ (cm)	Receiver Type	Antenna Type	GPS Array
1	MEXI	5432	338.03	5.13	87.46	112.7	TRIMBLE 5700	TRM41249.00	RGNA
2	CULI	2747	301.83	4.16	110.83	115.2	TRIMBLE 5700	TRM41249.00	RGNA
3	LPAZ	5909	271.16	9.24	99.47	104.7	TRIMBLE 5700	TRM41249.00	RGNA
4	MPR1	1652	106.36	61.67	93.10	4.33	NOV WAASGII	MPL WAAS 2225NW	CORS
5	CAYA	2136	106.07	3.49	40.56	17.14	LEICA SR530	TRM22020.00	UNAM
6	MTP1	1348	105.31	64.35	86.01	4.23	NOV WAASGII	MPL WAAS 2225NW	CORS
7	MSD1	1623	97.35	60.18	81.46	3.84	NOV WAASGII	MPL WAAS 2225NW	CORS
8	SA61	637	93.32	39.16	44.17	8.19	TRIMBLE 4700	TRM33429.20	SNG
9	INEG	3704	85.56	4.44	17.45	20.4	TRIMBLE 5700	TRM29659.00	RGNA
10	DOAR	1435	85.48	3.32	55.29	24.32	ASHTECH UZ12	ASH701945E_M	UNAM
11	MMD1	1655	84.26	55.81	71.19	1.92	NOV WAASGII	MPL WAAS 2225NW	CORS
12	CIC1	1083	74.33	15.82	20.91	5.90	ROGUE SNR8000	AOAD/M_T	SCIGN
13	MMX1	1639	69.57	50.99	59.56	1.80	NOV WAASGII	MPL WAAS 2225NW	CORS
14	CORX	1387	67.58	8.06	49.84	12.81	ASHTECH ZII3	ASH701945C_M	SCIGN
15	YAIG	1181	59.79	3.45	35.92	11.64	ASHTECH ZII3	ASH700936E_C	UNAM
16	IITJ	2898	55.02	34.79	46.20	1.54	TRIMBLE 4400	TRM23903.00	RGNA
17	OXEC	498	53.15	36.82	38.98	2.59	TRIMBLE NETRS	TRM41249.00	SNG
18	IMIE	342	52.09	25.84	36.70	2.24	TRIMBLE NETR9	TRM55971.00	RGNA
19	GUAX	973	50.85	34.27	39.00	1.11	ASHTECH ZII3	ASH701945C_M	SCIGN
20	SPMX	216	46.56	36.58	43.09	1.68	ASHTECH ZII3	ASH701945B_M	SCIGN
21	PHJX	428	43.65	38.18	41.20	0.61	TRIMBLE NETR9	TRM59800.00	PBO
22	UCOM	460	38.01	32.41	34.75	0.85	TRIMBLE NETRS	TRM41249.00	SNG
23	USMX	1468	37.87	29.94	31.86	0.81	TRIMBLE NETRS	ASH701945B_M	SCIGN
24	SG21	1071	37.42	27.83	30.42	1.62	TRIMBLE 4700	TRM33429.20	SNG
25	CHET	2622	36.03	9.28	15.38	3.98	TRIMBLE 5700	TRM41249.00	RGNA
26	VIL2	1062	35.71	12.65	16.28	3.35	TRIMBLE 5700	TRM41249.00	RGNA
27	CULC	1074	35.63	10.12	13.82	1.55	TRIMBLE 5700	TRM41249.00	RGNA
28	HER2	3581	35.23	6.73	14.94	2.82	TRIMBLE 5700	TRM41249.00	RGNA
29	YESX	181	35.21	32.78	33.76	0.43	TRIMBLE NETRS	ASH701945B_M	SCIGN
30	COL2	2622	34.64	11.80	19.02	6.15	TRIMBLE 5700	TRM41249.00	RGNA
31	TOL2	2612	33.95	5.39	12.85	3.66	TRIMBLE 5700	TRM41249.00	RGNA
32	UQRO	711	33.82	18.58	24.39	2.27	ASHTECH ZII3	ASH700228D	RGNA
33	IDGO	1065	33.76	26.73	30.12	0.70	ASHTECH ZII3	ASH700228D	RGNA
34	MTY2	2627	33.04	6.20	12.88	2.20	TRIMBLE 5700	TRM41249.00	RGNA
35	MERI	2637	32.64	8.10	12.90	3.01	TRIMBLE 5700	TRM41249.00	RGNA
36	PTEX	612	32.56	27.86	30.38	0.64	TRIMBLE NETRS	TRM59800.00	PBO
37	OAX2	2629	32.23	4.39	12.78	2.66	TRIMBLE 5700	TRM41249.00	RGNA
38	IMIP	1034	32.2	29.81	30.87	0.46	TRIMBLE 5700	TRM41249.00	RGNA
39	CAM2	1152	31.90	5.32	12.68	3.19	TRIMBLE 5700	TRM41249.00	RGNA
40	TAMP	1049	30.91	11.40	15.23	1.94	TRIMBLE 5700	TRM41249.00	RGNA
41	ICAM	1086	30.72	10.39	14.05	3.50	TRIMBLE 5700	TRM41249.00	RGNA
42	CHI3	1087	30.62	9.33	13.28	1.82	TRIMBLE 5700	TRM41249.00	RGNA
43	PLTX	792	30.45	27.76	28.97	0.45	TRIMBLE NETRS	TRM29659.00	PBO
44	ICEP	1004	29.75	17.76	20.59	1.31	ASHTECH ZII3	ASH700228D	RGNA
45	USLP	1042	29.18	19.54	23.62	1.07	ASHTECH ZII3	ASH700228D	RGNA
46	PALX	728	29.04	25.68	26.83	0.44	TRIMBLE NETRS	TRM59800.00	PBO
47	UGTO	1063	28.62	7.99	12.01	2.51	TRIMBLE 5700	TRM41249.00	RGNA
48	PSTX	850	27.43	24.21	25.71	0.49	TRIMBLE NETRS	TRM59800.00	PBO
49	PJZX	686	26.79	24.99	25.48	0.21	TRIMBLE NETRS	TRM59800.80	PBO
50	PTAX	609	25.82	23.21	23.94	0.37	TRIMBLE NETRS	ASH701945B_M	PBO
51	UVER	229	25.25	11.76	14.06	1.83	ASHTECH ZII3	ASH700228D	RGNA
52	PLPX	794	22.40	21.10	21.52	0.18	TRIMBLE NETRS	TRM59800.80	PBO
53	IPAZ	346	19.85	11.95	14.83	1.13	TRIMBLE 5700	TRM41249.00	RGNA

**Table 3. Statistics of the MP2-RMS variations for CGPS sites spanning Mexico.**

Rank (Order)	Site	No. of Days	Max (cm)	Min (cm)	Mean (cm)	St. Dev. $\pm$ (cm)	Receiver Type	Antenna Type	GPS Array
1	CAYA	2136	216.43	7.64	55.77	31.32	LEICA SR530	TRM22020.00	UNAM
2	IITJ	2898	129.14	49.73	98.02	7.11	TRIMBLE 4400	TRM23903.00	RGNA
3	MPR1	1652	120.62	73.64	101.44	4.38	NOV WAASGII	MPL WAAS 2225NW	CORS
4	MTP1	1348	109.44	72.04	94.97	4.76	NOV WAASGII	MPL WAAS 2225NW	CORS
5	MSD1	1623	104.01	61.71	90.53	4.55	NOV WAASGII	MPL WAAS 2225NW	CORS
6	SA61	637	92.28	42.62	46.93	7.32	TRIMBLE 4700	TRM33429.20	SNG
7	CIC1	1083	91.52	52.41	60.06	3.87	ROGUE SNR8000	AOAD/M_T	SCIGN
8	MMD1	1655	86.92	57.17	79.14	2.49	NOV WAASGII	MPL WAAS 2225NW	CORS
9	DOAR	1435	85.18	6.79	57.49	21.12	ASHTECH UZ12	ASH701945E_M	UNAM
10	YAIG	1181	85.00	8.14	42.76	11.45	ASHTECH ZII3	ASH700936E_C	UNAM
11	LPAZ	5909	74.79	20.89	39.65	12.1	TRIMBLE 5700	TRM41249.00	RGNA
12	CORX	1387	72.85	9.57	48.61	14.41	ASHTECH ZII3	ASH701945C_M	SCIGN
13	MEXI	5432	70.86	12.82	34.94	14.6	TRIMBLE 5700	TRM41249.00	RGNA
14	MMX1	1639	69.88	50.36	58.90	1.35	NOV WAASGII	MPL WAAS 2225NW	CORS
15	IMIE	342	65.28	39.08	45.10	2.11	TRIMBLE NETR9	TRM55971.00	RGNA
16	COL2	2622	60.82	31.56	40.65	7.26	TRIMBLE 5700	TRM41249.00	RGNA
17	IDGO	1065	55.54	41.57	48.16	1.72	ASHTECH ZII3	ASH700228D	RGNA
18	CHET	2622	54.54	19.35	26.88	4.39	TRIMBLE 5700	TRM41249.00	RGNA
19	CULI	2747	54.31	4.17	26.34	17.56	TRIMBLE 5700	TRM41249.00	RGNA
20	INEG	3704	54.16	10.06	26.01	12.3	TRIMBLE 5700	TRM29659.00	RGNA
21	GUAX	973	54.05	35.13	41.83	1.42	ASHTECH ZII3	ASH701945C_M	SCIGN
22	OXEC	498	53.40	39.80	42.04	2.10	TRIMBLE NETRS	TRM41249.00	SNG
23	IMP	1034	51.94	45.07	47.70	0.84	TRIMBLE 5700	TRM41249.00	RGNA
24	OAX2	2629	51.63	7.90	19.84	4.54	TRIMBLE 5700	TRM41249.00	RGNA
25	PHJX	428	50.64	46.26	49.13	0.44	TRIMBLE NETR9	TRM59800.00	PBO
26	SPMX	216	50.53	40.31	46.39	2.08	ASHTECH ZII3	ASH701945B_M	SCIGN
27	VIL2	1062	50.43	24.84	29.69	3.76	TRIMBLE 5700	TRM41249.00	RGNA
28	CULC	1074	48.37	24.59	28.37	1.59	TRIMBLE 5700	TRM41249.00	RGNA
29	TOL2	2612	46.79	11.88	22.26	4.03	TRIMBLE 5700	TRM41249.00	RGNA
30	UCOM	460	46.74	40.41	43.28	1.06	TRIMBLE NETRS	TRM41249.00	SNG
31	HER2	3581	46.49	12.00	28.08	3.70	TRIMBLE 5700	TRM41249.00	RGNA
32	TAMP	1049	46.13	23.70	27.26	2.34	TRIMBLE 5700	TRM41249.00	RGNA
33	MERI	2637	45.89	17.00	26.32	3.17	TRIMBLE 5700	TRM41249.00	RGNA
34	MTY2	2627	44.86	12.30	21.41	2.42	TRIMBLE 5700	TRM41249.00	RGNA
35	ICAM	1086	44.19	20.50	25.94	3.74	TRIMBLE 5700	TRM41249.00	RGNA
36	ICEP	1004	42.92	24.96	29.01	2.11	ASHTECH ZII3	ASH700228D	RGNA
37	SG21	1071	42.70	27.87	33.93	2.80	TRIMBLE 4700	TRM33429.20	SNG
38	CHI3	1087	42.62	21.89	24.85	2.01	TRIMBLE 5700	TRM41249.00	RGNA
39	UQRO	711	41.80	20.06	27.85	3.93	ASHTECH ZII3	ASH700228D	RGNA
40	CAM2	1152	41.36	11.67	19.01	3.59	TRIMBLE 5700	TRM41249.00	RGNA
41	PLTX	792	39.55	36.74	38.30	0.49	TRIMBLE NETRS	TRM29659.00	PBO
42	PTEX	612	39.45	34.82	37.69	0.85	TRIMBLE NETRS	TRM59800.00	PBO
43	USMX	1468	38.74	33.06	34.73	0.69	TRIMBLE NETRS	ASH701945B_M	SCIGN
44	YESX	181	38.44	34.77	36.85	0.77	TRIMBLE NETRS	ASH701945B_M	SCIGN
45	USLP	1042	37.66	23.24	30.33	1.44	ASHTECH ZII3	ASH700228D	RGNA
46	IPAZ	346	37.60	25.86	29.38	1.63	TRIMBLE 5700	TRM41249.00	RGNA
47	PSTX	850	36.85	30.24	33.86	1.23	TRIMBLE NETRS	TRM59800.00	PBO
48	UVER	229	35.31	16.69	19.31	2.36	ASHTECH ZII3	ASH700228D	RGNA
49	PALX	728	34.36	29.83	32.52	0.80	TRIMBLE NETRS	TRM59800.00	PBO
50	UGTO	1063	32.13	11.73	17.52	3.06	TRIMBLE 5700	TRM41249.00	RGNA
51	PJZX	686	31.73	28.62	30.25	0.61	TRIMBLE NETRS	TRM59800.80	PBO
52	PTAX	609	29.60	26.63	28.05	0.44	TRIMBLE NETRS	ASH701945B_M	PBO
53	PLPX	794	24.33	22.93	23.64	0.26	TRIMBLE NETRS	TRM59800.80	PBO

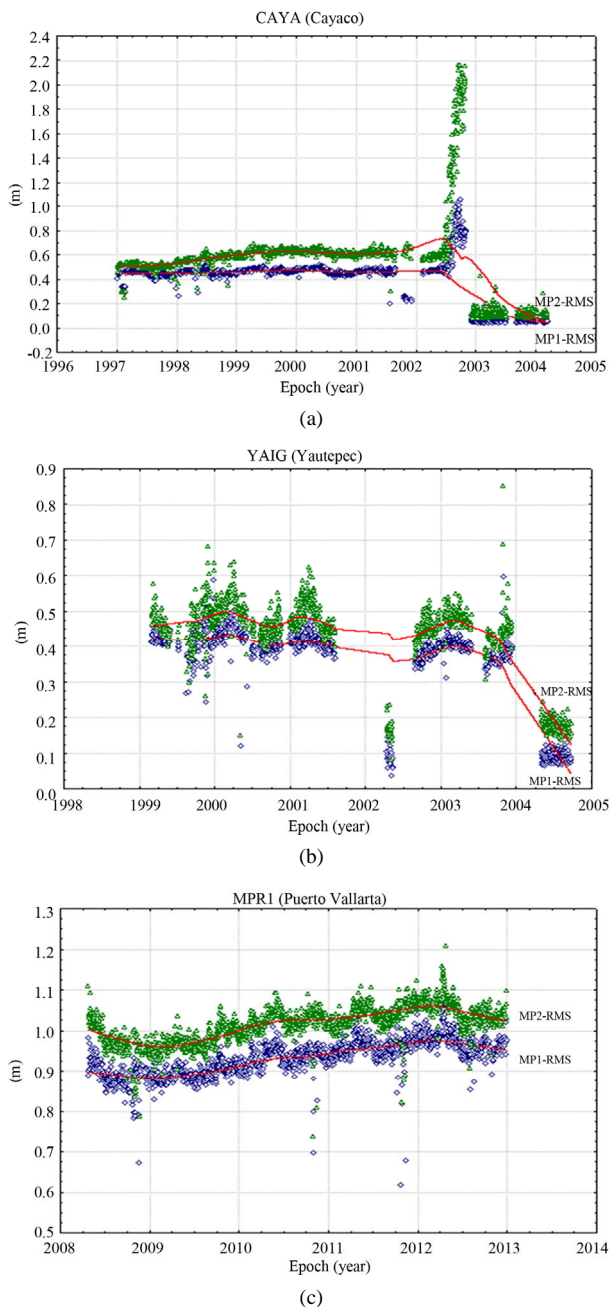


**Figure 10. Pseudorange multipath (MP1-RMS and MP2-RMS) variations, most affected sites: (a) Cayaco (CAYA) and Yautepec (YAIG), UNAM network and (c) Puerto Vallarta (MPR1), CORS network.**

ranging from almost one to several years.

## 5. Conclusion

Based on the presented pseudorange assessment and analysis, it can be concluded that MEXI, CULI and LPAZ sites, as part of the RGNA network, were the three most affected (meter level) on the MP1-RMS results. However, recalling that prior to 2000, there was only

C/A code available for these stations, there was no solution for the MP2-RMS and the only solution reported for the MP1-RMS was based on this code. After 2000, and derived from the MP2-RMS results, these sites reduced their rank amongst all stations to 11<sup>th</sup>, 13<sup>th</sup> and 19<sup>th</sup> highest, respectively. In addition, the cooperative station belonging to the RGNA network and controlled by the IITJ was positioned 16<sup>th</sup> and 2<sup>nd</sup>, while INEGI's site, which was the only station of the RGNA that used a Trimble Choke-Ring antenna was ranked 9<sup>th</sup> and 20<sup>th</sup>, respectively. On the other hand, site CAYA that belongs to the UNAM network was considered as one of the most affected sites; ranking in 1<sup>st</sup> place for the MP2-RMS and 5<sup>th</sup> for the MP1-RMS. Sites SA61 and YAIG from the SNG and UNAM networks respectively, as well as all the sites from the CORS network were located within the top fifteen sites for highest MP1-RMS and MP2-RMS values. The least affected CGPS sites (PLPX, PTAX and PJZX) belong to the PBO network; they experienced the smallest amounts of pseudorange multipath among all stations for MP2-RMS, and in the lowest 10 percent for MP1-RMS. Possible reasons for high multipath at some of the analyzed CGPS stations can be attributed to issues related to GPS hardware replacement (*i.e.*, receiver and antenna type or receiver firmware version), to the existence of the antenna radome, and/or the antenna environment (vegetation, constructions, local structures and rocks). The annual seasonal effect for the pseudorange multipath vs. height variations (presented in the form of time-series) shows a reasonable level of agreement or coincidence between these two types of solutions; however, this issue requires further investigation. It is expected that pseudorange multipath can be used for further data cleaning to improve positioning results, together with an assessment of ionospheric and tropospheric effects and carrier phase multipath.

## 6. Acknowledgements

The authors would like to thank UNAVCO, PBO, INEGI, IITJ, SCIGN, USGS, JPL, UNAM, SNG and CORS networks, for making the GPS data publicly available for the analysis. This research is funded by a postdoctoral scholarship (186766) from the National Council of Science and Technology (CONACYT).

## REFERENCES

- [1] A. Bilich and K. M. Larson, "Mapping the GPS Multipath Environment Using the Signal-to-Noise Ratio (SNR)," *Radio Science*, Vol. 42, No. 6, 2007, pp. 1-16. [doi:10.1029/2007RS003652](https://doi.org/10.1029/2007RS003652)
- [2] P. Elósegui, J. L. Davis, R. K. Jaldehag, J. M. Johansson, A. E. Niell and I. I. Shapiro, "Geodesy Using the Global Positioning System: The Effects of Signal Scattering on

- Estimates of Site Position,” *Journal of Geophysical Research: Solid Earth*, Vol. 100, No. B6, 1995, pp. 9921-9934. [doi:10.1029/95JB00868](https://doi.org/10.1029/95JB00868)
- [3] L. Estey and C. M. Meertens, “TEQC: The Multi-Purpose Toolkit for GPS/GLONASS Data,” *GPS Solutions*, Vol. 3, No. 1, 1999, pp. 42-49. [doi:10.1007/PL00012778](https://doi.org/10.1007/PL00012778)
- [4] L. L. Ge, S. W. Han and C. Rizos, “Multipath Mitigation of Continuous GPS Measurements Using an Adaptive Filter,” *GPS Solutions*, Vol. 4, No. 2, 2000, pp. 19-30. [doi:10.1007/PL00012838](https://doi.org/10.1007/PL00012838)
- [5] L. L. Ge, S. W. Han and C. Rizos, “GPS Multipath Change Detection in Permanent GPS Stations,” *Survey Review*, Vol. 36, No. 283, 2002, pp. 306-322. [doi:10.1179/003962602791483271](https://doi.org/10.1179/003962602791483271)
- [6] S. Hilla and M. Cline, “Evaluating Pseudorange Multipath Effects at Stations in the National CORS Network,” *GPS Solutions*, Vol. 8, No. 4, 2004, pp. 253-267. [doi:10.1007/s10291-003-0073-3](https://doi.org/10.1007/s10291-003-0073-3)
- [7] M. A. King and C. S. Watson, “Long GPS Coordinate Time Series: Multipath and Geometry Effects,” *Journal of Geophysical Research: Solid Earth*, Vol. 115, No. B4, 2010. [doi:10.1029/2009JB006543](https://doi.org/10.1029/2009JB006543)
- [8] K. M. Larson, E. Gutmann, V. Zavorotny, J. Braun, M. Williams and F. Nievinski, “Can We Measure Snow Depth with GPS Receivers?” *Geophysical Research Letters*, Vol. 36, No. 17, 2009, pp. 1-5. [doi:10.1029/2009GL039430](https://doi.org/10.1029/2009GL039430)
- [9] A. R. Lowry, K. M. Larson, V. Kostoglodov and R. Bilham, “Transient Fault Slip in Guerrero, Southern Mexico,” *Geophysical Research Letters*, Vol. 28, No. 19, 2001, pp. 3753-3756. [doi:10.1029/2001GL013238](https://doi.org/10.1029/2001GL013238)
- [10] K. D. Park, P. Elósegui, J. L. Davis, P. O. J. Jarlemark, B. E. Corey, A. E. Niell, J. E. Normandeau, C. E. Meertens, and V. A. Andreatta, “Development of an Antenna and Multipath Calibration System for Global Positioning System Sites,” *Radio Science*, Vol. 39, No. 5, 2004, pp. 1-13. [doi:10.1029/2003RS002999](https://doi.org/10.1029/2003RS002999)
- [11] R. Jim, “Systematic Errors in GPS Position Estimates,” *IGS Workshop 2006*, Darmstadt, 8-11 May 2006.
- [12] C. Rizos and S. W. Han, “Quality Control Issues in Real-time GPS Positioning,” *IUGG Congress*, Birmingham, 18-30 July 1999.
- [13] G. W. Roberts, X. Meng, A. H. Dodson and E. Cosser, “Multipath Mitigation for Bridge Deformation Monitoring,” *Journal of Global Positioning System*, Vol. 1, No. 1, 2002, pp. 25-33. [doi:10.5081/jgps.1.1.25](https://doi.org/10.5081/jgps.1.1.25)
- [14] C. Satirapod, R. Khoonphool and C. Rizos, “Multipath Mitigation of Permanent GPS Stations Using Wavelets,” *International Symposium on GPS/GNSS*, Tokyo, 15-18 November 2003, pp. 133-139.
- [15] E. E. Small, K. M. Larson and J. J. Braun, “Sensing Vegetation Growth with Reflected GPS Signals,” *Geophysical Research Letters*, Vol. 37, No. , 2010, pp. 1-5. [doi:10.1029/2010GL042951](https://doi.org/10.1029/2010GL042951)
- [16] G. E. Vázquez and D. A. Grejner-Brzeziska, “A Case Study for Pseudorange Multipath Estimation and Analysis: TAMDEF GPS Network,” *Geofísica Internacional*, Vol. 51, No. 1, 2012, pp. 63-72.
- [17] S. Yoshioka, T. Mikumo, V. Kostoglodov, K. M. Larson, A. R. Lowry and S. K. Singh, “Interplate Coupling and a Recent Aseismic Slow Slip Event in the Guerrero Seismic Gap of the Mexican Subduction Zone, as Deduced from GPS Data Inversion Using a Bayesian Information Criterion,” *Physics of the Earth and Planetary Interiors*, Vol. 146, No. 3-4, 2004, pp. 513-530. [doi:10.1016/j.pepi.2004.05.006](https://doi.org/10.1016/j.pepi.2004.05.006)
- [18] <http://facility.unavco.org/software/teqc/teqc.html>
- [19] UNAVCO, “QC v3 User Guide,” 1994. <http://www.unavco.org>
- [20] <http://pbo.unavco.org/station/overview/>
- [21] <http://www.inegi.org.mx/>
- [22] <http://usuarios.geofisica.unam.mx/>